Edge energy transport barrier and turbulence in the I-mode regime on Alcator C-Mod

Edge energy transport barrier and turbulence in the I-mode regime on Alcator C-Mod[a)]

A. E. Hubbard,[1,b)] D. G. Whyte,[1] R. M. Churchill,[1] I. Cziegler,[1] A. Dominguez,[1] T. Golfinopoulos,[1] J. W. Hughes,[1] J. E. Rice,[1] I. Bespamyatnov,[2] M. J. Greenwald,[1] N. Howard,[1] B. Lipschultz,[1] E. S. Marmar,[1] M. L. Reinke,[1] W. L. Rowan,[2] J. L. Terry,[1] and Alcator C-Mod Group

[1]*Plasma Science and Fusion Center, MIT, Cambridge, Massachusetts 02129, USA*

[2]*Fusion Research Center, University of Texas at Austin, Austin, Texas 78712, USA*

(Received 3 December 2010; accepted 1 March 2011; published online 19 May 2011)

We report extended studies of the I-mode regime [Whyte *et al.*, Nucl. Fusion **50**, 105005 (2010)] obtained in the Alcator C-Mod tokamak [Marmar *et al.*, Fusion Sci. Technol. **51**(3), 3261 (2007)]. This regime, usually accessed with unfavorable ion $B \times \nabla B$ drift, features an edge thermal transport barrier without a strong particle transport barrier. Steady I-modes have now been obtained with favorable $B \times \nabla B$ drift, by using specific plasma shapes, as well as with unfavorable drift over a wider range of shapes and plasma parameters. With favorable drift, power thresholds are close to the standard scaling for L–H transitions, while with unfavorable drift they are ~ 1.5–3 times higher, increasing with I_p. Global energy confinement in both drift configurations is comparable to H-mode scalings, while density profiles and impurity confinement are close to those in L-mode. Transport analysis of the edge region shows a decrease in edge χ_{eff}, by typically a factor of 3, between L- and I-mode. The decrease correlates with a drop in mid-frequency fluctuations ($f \sim 50$–150 kHz) observed on both density and magnetics diagnostics. Edge fluctuations at higher frequencies often increase above L-mode levels, peaking at $f \sim 250$ kHz. This weakly coherent mode is clearest and has narrowest width ($\Delta f/f \sim 0.45$) at low q_{95} and high T_{ped}, up to 1 keV. The E_r well in I-mode is intermediate between L- and H-mode and is dominated by the diamagnetic contribution in the impurity radial force balance, without the V_{pol} shear typical of H-modes. © *2011 American Institute of Physics*. [doi:10.1063/1.3582135]

I. INTRODUCTION

The high confinement, or H-mode regime, has been observed in tokamaks and other magnetic confinement devices for over 25 years.[1] It is characterized by edge transport barriers in both energy and particle channels, as evidenced by the formation of a narrow region of steep temperature and density gradient (or "pedestal") at and inboard of the last closed flux surface (LCFS), a sudden decrease in the H_α or D_α emission, and increases in average density and stored energy. Turbulence in the edge region typically decreases suddenly, which is thought to be responsible for the decreasing local transport. The global energy confinement increases considerably, by typically a factor of two compared to the low confinement L-mode regime without a barrier. This has greatly advanced prospects for fusion by reducing the device size needed to achieve a given confinement time. H-mode is the standard operating regime for most divertor tokamaks, including Alcator C-Mod,[2] and foreseen for ITER.[3] However, it is becoming increasingly clear that issues associated with H-mode pose operational challenges in a burning plasma. With a quiescent particle barrier, both electron density and impurity content continuously increase, until either the temperature pedestal erodes through core radiation, or a pressure limit is reached. Some edge instability is thus required to increase particle transport and regulate pressure. The most common such instabilities, large type I edge localized modes (ELMs),[4] release substantial energy which would erode or melt material surfaces;[5] these must either be actively mitigated or replaced with more benign, continuous instabilities such as the quasicoherent (QC) mode in enhanced D_α (EDA) H-mode[6] or the edge harmonic oscillation in quiescent H-mode.[7] High particle confinement is also problematic in terms of transporting helium "ash" out of a burning plasma, and accumulating impurities in the core, diluting the fusion fuel. Independent control of energy and particle transport barriers would be ideal. The challenge is to avoid ELMs and impurity accumulation while also maintaining confinement and pressure sufficient for a burning regime.

A regime of operation has recently been explored on the Alcator C-Mod tokamak, referred to as "improved mode" or I-mode, which features an edge thermal transport barrier *without* a significant reduction in particle transport.[8,9] It is characterized by steepening of ion and electron temperature gradients, comparable to those in H-mode, while density profiles remain close to those in L-mode [Fig. 1(a)]. As can be seen in Fig. 1(b), stored energy also increases, while density remains constant, and there is only a modest change in D_α, all in notable contrast to H-mode. Radiated power, not shown, is also unchanged.

Historically, modest increases in edge temperature and confinement were observed, usually transiently, in discharges with ion $B \times \nabla B$ drift away from the active x-point,

[a)]Paper PI2 6, Bull. Am. Phys. Soc. 55, 239 (2010).
[b)]Invited speaker.

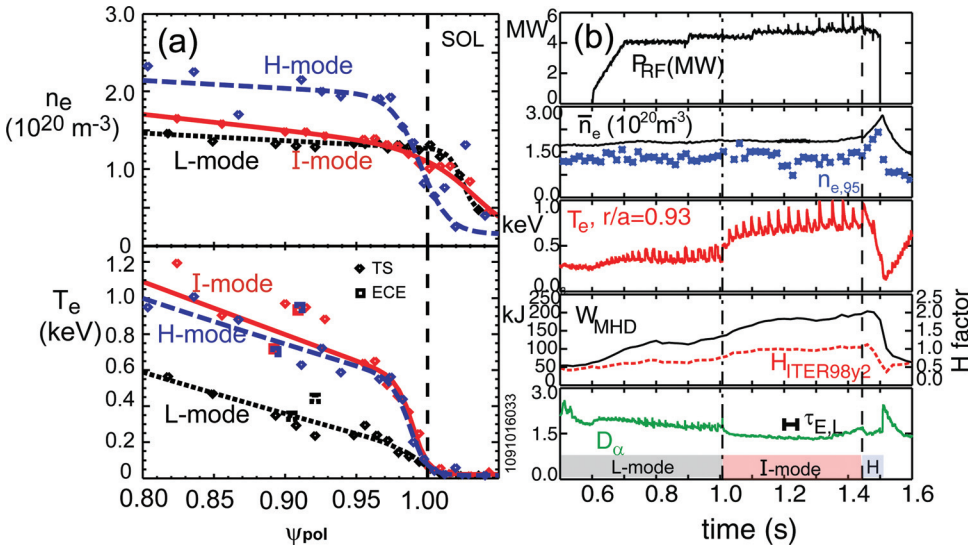

FIG. 1. (Color online) (a) Edge profiles of electron density (top) and temperature (bottom) for different phases of a 1.27 MA, 5.6 T C-Mod discharge (1091016033). Curves have been fit using a modified tan*h* function as described in Ref 28. The I-mode phase (red solid line, 1.41 s) has a steep T_e gradient, but a density profile close to that in L-mode (black dotted line, 0.78 s). In a brief ELM-free H-mode (blue dashed curve, 1.47 s) T_e is similar to I-mode but n_e is much steeper. (b) Time histories of input ICRF power (top) and plasma parameters for the same discharge. In fourth panel, solid black curve is stored energy, and dashed red curve is confinement normalized to IPB98y2 scaling, reaching 1 in I-mode (Ref. 18).

which is known to increase the H-mode power threshold.[10–12] This phenomenon was termed "improved L-mode" on ASDEX Upgrade.[11,13] It was shown that due to profile stiffness, global confinement also improved.[10] As edge profile and fluctuation diagnostics improved, it was noted that changes in broadband fluctuation spectra accompanied the reduction in edge transport, with decreases at moderate f and increases at $f > 150$ kHz.[14]

Recent C-Mod experiments have greatly extended I-mode phases in both duration and performance, establishing this as a distinct, stationary transport barrier regime in which energy and particle transport are clearly separated. Steady I-modes have been maintained for >20 energy confinement times, in some cases limited only by the duration of the heating power and discharge flat top. Both normalized energy confinement and stored energy are comparable to those in C-Mod H-modes,[10] and the regime has been studied over a wide range of plasma parameters ($0.7 \le I_p \le 1.3$ MA, $3 \le B_T \le 6$ T, $0.86 \le \bar{n}_e \le 2.05 \times 10^{20}$ m^{-3}) (Ref. 9). Volume averaged pressure, up to 1.5 atm, has approached the C-Mod, and tokamak, H-mode record of 1.8 atm. Newer experiments have demonstrated that steady I-modes can also be reliably accessed, in a lower power range, with favorable $B \times \nabla B$ drift in certain plasma shapes. The behavior, access conditions, and confinement in this configuration are described, and compared to those in unfavorable drift configuration, in Sec. II. Measurements and analysis of the edge plasma transport and the turbulence, flows, and electric field profiles which are thought to underlie the differences in energy and particle transport between L-, I-, and H-mode are presented in Sec. III. Transport questions raised by these observations, key issues for the application of the I-mode in burning plasmas, and directions for future work are discussed in Sec. IV. Section V summarizes the conclusions of the present study.

II. COMPARISON OF I-MODES WITH FAVORABLE AND UNFAVORABLE $B \times B$ DRIFT

Most I-modes on C-Mod, as well as improved L-modes elsewhere, were obtained with ion $B \times \nabla B$ drift away from the active x-point. For C-Mod this can be achieved either by reversing the magnetic field and current for discharges with dominant x-points near the closed lower divertor, or in a "normal" field with an x-point near the open upper divertor. A typical separatrix shape in this configuration is shown by the red curve in Fig. 2, though I-modes have been achieved in a range of shapes (elongation $k = 1.5$–1.78, triangularity $\delta = 0.3$–0.85 in the direction of the active x-point, average $\delta = 0.35$–0.6).

Transient examples of I-mode-like behavior with favorable drift were first noted unexpectedly in the pre-H-mode phases of a discharge in the LSN shape shown in green in Fig 2.[9] Further experiments in 2010 have confirmed that

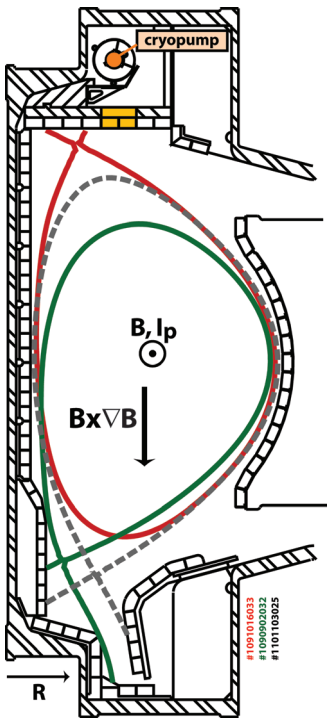

FIG. 2. (Color online) Typical shape of C-Mod last closed flux surface for I-mode experiments in unfavorable drift (upper x-point) and favorable drift (lower x-point, solid). Plasmas in more usual C-mod configurations (e.g., dashed gray curve) have not exhibited transitions to I-mode.

I-mode can be robustly accessed in this shape, and be extended to steady state (>10 τ_E). As shown in Fig. 3, these I-mode discharges exhibit typical turbulence signatures of the regime, namely a reduction in mid-frequency fluctuations, 70–150 kHz in this example, and a simultaneous increase in higher frequency fluctuations, with a "weakly coherent mode" peaking at 230–250 kHz. Density and radiation remain steady for the duration of the ion cyclotron resonance heating (ICRH), with no ELMs. These experiments were conducted at 5.4–5.55 T, with I_p 0.8–1.0 MA (q_{95} 3.1–3.9), and I-mode access was found to be sensitive to the x-point radius and/or strike point location. It should be emphasized that the formation of a thermal barrier before an H-mode transition is not normally observed in more typical shapes with favorable drift (e.g., the dashed curve in Fig. 2), even when power is ramped slowly[15,16] or power thresholds are high due to high B (Ref. 14); broadband turbulence, particle and energy transport generally decrease promptly and simultaneously at L–H transitions. However, transitions have not been studied in all potential shapes with favorable drift, so it is possible that I-mode can be accessed in other shapes.

The biggest difference in I-modes with favorable vs. unfavorable magnetic configuration is in the lower power range for which the regime is accessed and can be sustained. Figure 4(a) shows the total loss power $P_{loss} = P_{RF,abs} + P_{oh} - dW/dt$, where $P_{RF,abs}$ is the absorbed ICRF power, estimated as 80% of the coupled power, P_{oh} is the ohmic input power, which often decreases in I-mode, and W is the stored energy. Time windows are selected just before L–I transitions (red squares), representing the lower power threshold in a given discharge, and prior to I–H transitions, representing the upper limit of the regime for a given discharge (black squares). In some of the favorable drift cases, where the transition time was not distinct, windows early in the I-mode phase were used, giving an upper bound on P_{L-I}. Power is normalized to the recent International Tokamak Physics Activity (ITPA) scaling,[17] $P_{Thresh} = 0.0488\ n_{e20}^{0.717}\ B_T^{0.80}\ S^{0.941}$, which was developed for favorable drift configurations. Not surprisingly, I–H thresholds for the unfavorable configuration are significantly higher. They also exhibit a strong I_p or q_{95} dependence, not present in the scaling, such that $P_{I-H}/P_{scaling}$ increases from an average of 1.4 at $q_{95} > 4.5$ to over 3 at $q_{95} < 3$. Thresholds for L–I transitions lie in a similar range and again increase with I_p; loss powers range from 1.9 to 5.7 MW. In contrast, discharges with favorable $B \times \nabla B$ drift have thresholds for both I–H and L–I thresholds which closely fit the standard L–H scaling, and there is no apparent q_{95} dependence. However, coil and power supply limitations restrict the range of plasma currents which can be achieved in this atypical shape to ≤1 MA, hence the range of q_{95} is more limited. P_{loss} in these I-modes is 1.1–1.6 MW. For 1 MA discharges, only 0.3 MW of ICRH was required. In a given discharge with varying ICRF power, the transition to I-mode is achieved at lower ICRF power than H-mode. Figure 1 shows a typical threshold experiment in which ICRF was deliberately increased in order to access both regimes; in other discharges with power kept constant, I-mode is maintained for the duration of the heating. However, partly due to evolution of ohmic power and dW/dt, there is considerable scatter in the total threshold powers for both L–I and I–H mode transitions, and a overlap in the P_{loss} ranges for which I and H-modes are accessed [Fig. 4(a)]. This indicates that, as has been seen for many years with

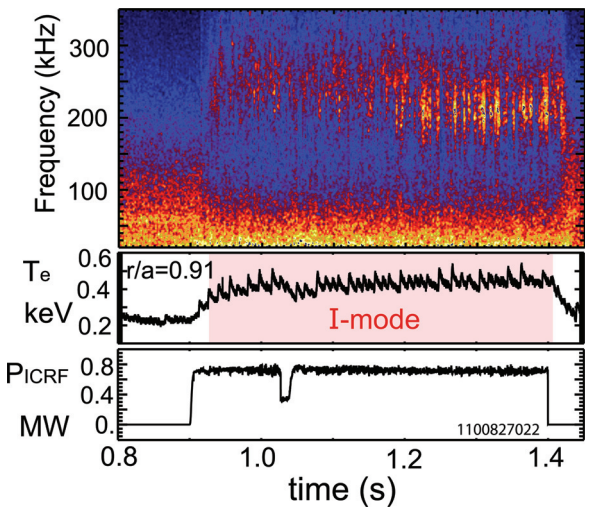

FIG. 3. (Color online) Steady I-mode achieved in favorable configuration (C-Mod discharge 1100827022, 0.8 MA, 5.4 T, lower single null). Density fluctuations measured by O-mode reflectometry (top panel), at $n_c = 7 \times 10^{19}$ m^{-3} ($r_c/a \cong 0.98$), show a decrease in mid-frequency turbulence and the appearance of a broad high f feature soon after the application of 0.75 MW ICRH (bottom). The I-mode phase, which has edge T_e significantly above that in similar L-mode discharges (middle panel), lasts for the duration of the RF pulse, about 10 τ_E.

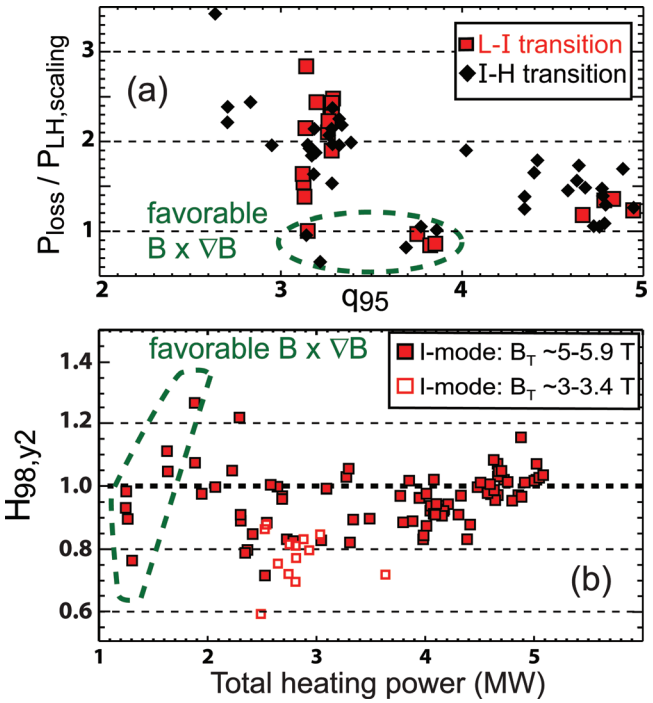

FIG. 4. (Color online) (a) Power thresholds for the L–I transition (red squares) and I–H transition (black diamonds), normalized to the Martin scaling (Ref. 17). The circled points are for favorable configuration and fit the scaling, while the remaining points, in unfavorable drift, are significantly higher. (b) Energy confinement time for I-mode discharges, normalized to the IPB98y2 scaling (Ref. 18). Average H_{98} is about 1, in both configurations, for discharges with $B_T > 5$ T (closed symbols) and about 0.8 for $B < 3.5$ T (open symbols).

H-modes, other variables must affect I-mode access. There appear to be optimum shapes[9] and ranges of density, although these parameters have not been systematically explored nor their importance is understood.

I-mode plasmas with favorable $B \times \nabla B$ drift direction also have similar normalized energy confinement to those with unfavorable drift and to H-modes. Figure 4(b) compares confinement times normalized to the IPB98(y2) scaling.[18] For comparison, $H_{98,y2}$ is typically in the range 0.7–1.1 for steady EDA or ELMy H-modes on C-Mod,[19] which were used in the IPB scaling. It can be higher for ELM-free H-modes, which however can only be maintained transiently. $H_{98,y2}$ for the I-modes with favorable drift ranges from 0.8 to 1.25, with an average about 1 as is also the case for previous 5–5.9 T I-modes. Due to the lower input power, however, absolute performance in this configuration is considerably lower, with maximum $T_{e,95}$ 0.57 keV and stored energy 95 kJ vs. 1.0 keV and 209 kJ in the highest power upper single null I-modes. The reduced power threshold is thus both an advantage, in that access to I-mode is easier, and a limitation. Because C-Mod is a high field, compact tokamak, the achieved pressure in both I and H-mode is generally not MHD-limited, even at the very high input power densities of up to 5.5 MW/m^3 (average power flux P/A $\leq$ 0.75 MW/m^2) used in these experiments. Normalized pressure β_N in I-modes to date is in the range 0.5–1.2, with the discharges in favorable drift at the lower end of the range. This compares with a range of $\sim$0.8–1.6 for most C-Mod H-modes; the maximum to date is $\beta_N = 1.8$ at 5.4 T, slightly higher at reduced B. Expanding the power range for robust I-modes, in both magnetic configurations, is a focus of current research.

III. EVOLUTION OF EDGE TURBULENCE AND TRANSPORT

A. Decrease of edge thermal transport and correlation with turbulence changes

Characteristic changes in broadband turbulence are distinctive features of the I-mode regime.[9] A typical example is shown in Fig. 5, for a discharge in the unfavorable configuration, which had clear transitions between L-mode, I-mode, and ELM-free H-mode at similar input power until 1.24 s, reverting to L-mode when ICRH decreased. Figure 5(a) shows the evolution of 88 GHz reflectometer spectra, sensitive to density fluctuations near $n_c = 9.6 \times 10^{19}$ m^{-3}, which for this period is at $r/a \cong 0.95$. A significant decrease in fluctuations is apparent at the L–I transition (1.07 s), in the frequency range 60–150 kHz. Beginning at the same time, turbulence peaks at higher frequencies, initially $\sim$200 kHz and gradually upshifting to $\sim$260 kHz as the T_e pedestal grows. At the I–H transition (1.22 s), remaining turbulence drops sharply at all $f > 20$ kHz, D_α drops, and density begins to rise sharply. Representative spectra in each regime are shown in Fig 5(e). In the I-mode phase (red), mid-frequency turbulence decreases to levels near H-mode, while the peak of the "weakly coherent mode" exceeds the L-mode level.

A simple thermal transport analysis has been carried out of the edge region, $0.95 \leq \psi \leq 1.0$, computing an effective

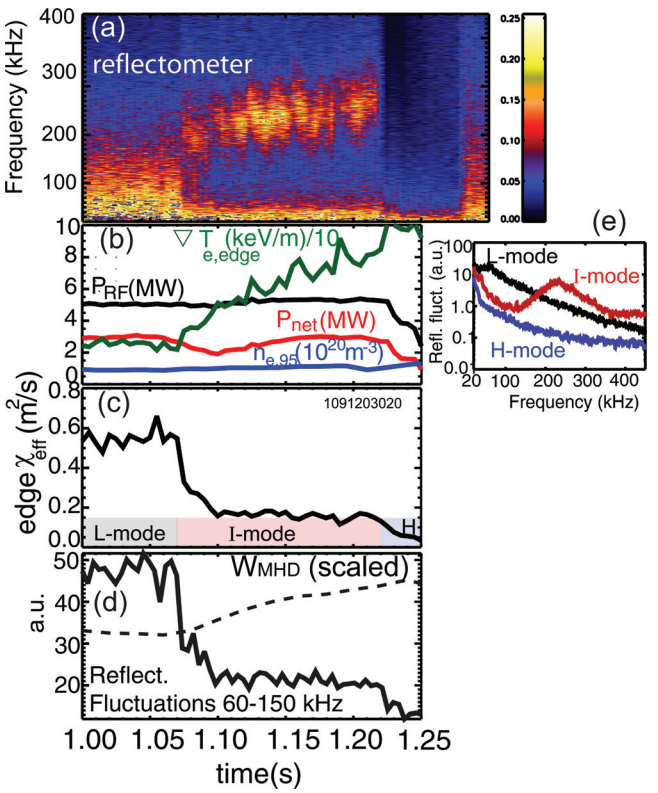

FIG. 5. (Color online) Fluctuations and edge thermal transport in L-, I-, and H-mode for a typical $q_{95} = 3.1$ C-Mod discharge 109120320 (1.3 MA, 5.8 T, upper single null). (a) Contours of reflectometer fluctuations (88 GHz, $n_c = 9.6 \times 10^{19}$ m^{-3} ($r_c/a \cong 0.95$) (b) Edge fluxes and gradients; ∇T_e ($0.95 < \psi < 1$)(green curve) increases from 25 to 88 keV/m in I-mode, whereas net power (red) drops slightly due to increasing dW/dt. (c) Computed χ_{eff} decreases from L-mode to I-mode, with a further reduction at the transition to an ELM-free H-mode. (d) Fluctuations integrated over the 60–150 kHz frequency band, exhibiting a decrease similar to that in χ_{eff}. Global stored energy (dashed line, scaled) increases during the I-mode phase as edge fluctuations and transport decrease. (e) Fluctuation spectra, averaged over 20 ms, in L-mode (1.03 s), I-mode (1.15 s), and H-mode (1.24 s).

thermal conductivity $\chi_{\text{eff}} = -P_{\text{net}}/(2\ \text{kA}\ n_e \nabla T_{\text{eff}})$, as described in Ref 15. ∇T_{eff} is derived using ECE measurements of T_e at ψ_{95} and edge Thomson scattering at the separatrix, with constraints for scrape-off layer power balance, assuming that power flux is split between electron and ion channels. While L-mode edge T_e profiles are typically linear, in I or H-mode ∇T_{eff} will be lower than the peak pedestal gradient. As shown in Fig 5(b), neither $P_{\text{net}} = P_{\text{loss}} - P_{\text{rad,core}}$, nor edge n_e, evaluated at mid-region from edge Thomson scattering,[20] is increasing significantly between L- and I-mode, while the average T_e gradient increases from 25 to 88 keV/m. χ_{eff} [Fig. 5(c)] thus decreases by a comparable percentage, from 0.55 to 0.2 m^2/s in the first 30 ms, with a slight further reduction at later times. Integrated reflectometer fluctuations in the 60–150 kHz band, shown in Fig 5(d), exhibit a decrease very similar in degree and time evolution, with a 60% drop in the first few milliseconds, and an 80% drop in the first 30 ms. This correlation strongly suggests that turbulence reduction in this band is responsible for the decreased thermal transport. However, it is notable that particle transport does not appear to change significantly. Fluctuations at higher frequency, in contrast, increase. At the I–H transition, there is a further decrease both in turbulence, at

all frequencies, and in χ_{eff}, which drops to about 0.05 m^2/s. In this period particle transport also appears reduced, though measurements of edge ionization (Ly_α) are not sufficient for a quantitative analysis in L- and I-mode.

While the general features of turbulence and transport changes are observed in all I-modes, the degree and rate of evolution are variable and depend on plasma parameters, in particular q_{95}. In some cases, particularly high current, low q_{95} discharges with large sawtooth heat pulses, a rapid transition from L- to I-mode occurs in only a few milliseconds, typically at a single heat pulse; see e.g., Fig. 15 of Ref. 9. At higher q_{95}, the transition can be more gradual and the turbulence peak at high frequencies broader and less pronounced. An example is shown in Fig. 6, with unfavorable drift and $q_{95} = 3.8$. In this case changes in turbulence begin soon after ICRH is turned on at 0.6 s, with edge T_e building up in steps at each sawtooth heat pulse. Mid-frequency turbulence [Fig. 6(d)] also decreases stepwise. It is interesting to note that an anticorrelation of edge T_e and turbulence exists even in the steady I-mode phase, suggesting that transient increases in edge T or ∇T due to heat pulses are further suppressing the turbulence. The high frequency peak in this case reaches but does not exceed the L-mode level [Fig. 6(e)], and is very broad. This discharge did not make a transition to H-mode but persisted in I-mode, except for a back-transition due to an impurity injection; a somewhat stronger and higher frequency weakly coherent mode was observed in the second I-mode phase [green curve in Fig. 6(e)]. In a few I-mode discharges at even higher q_{95} (4.7), a mid-frequency decrease was observed but there was no distinct higher frequency peak, rather a flattening of the fluctuation spectra.

While the decrease in mid-frequency turbulence is most clearly and consistently apparent on reflectometry, which is sensitive only to density fluctuations, at $k_\perp \leq 6$ cm^{-1}, and radially localized,[21] it is also observed on magnetics. Hence the responsible turbulence has an electromagnetic component. Sensitivity to plasma shape, particularly in the favorable configuration, also suggests a role for electromagnetic effects in the establishment of the I-mode regime. Fluctuations in the electron diamagnetic direction on the gas puff imaging (GPI) diagnostic, which views a puff of D or He gas at the outboard midplane,[22] typically decrease by a smaller degree, roughly 50%. D_α emission in the parameter range of I-mode pedestals is sensitive to both n_e and T_e. Since it is not yet clear whether there are also changes in T_e fluctuations, it is possible that perturbations in $\tilde{n}_e$ and $\tilde{T}_e$ are partially canceling.

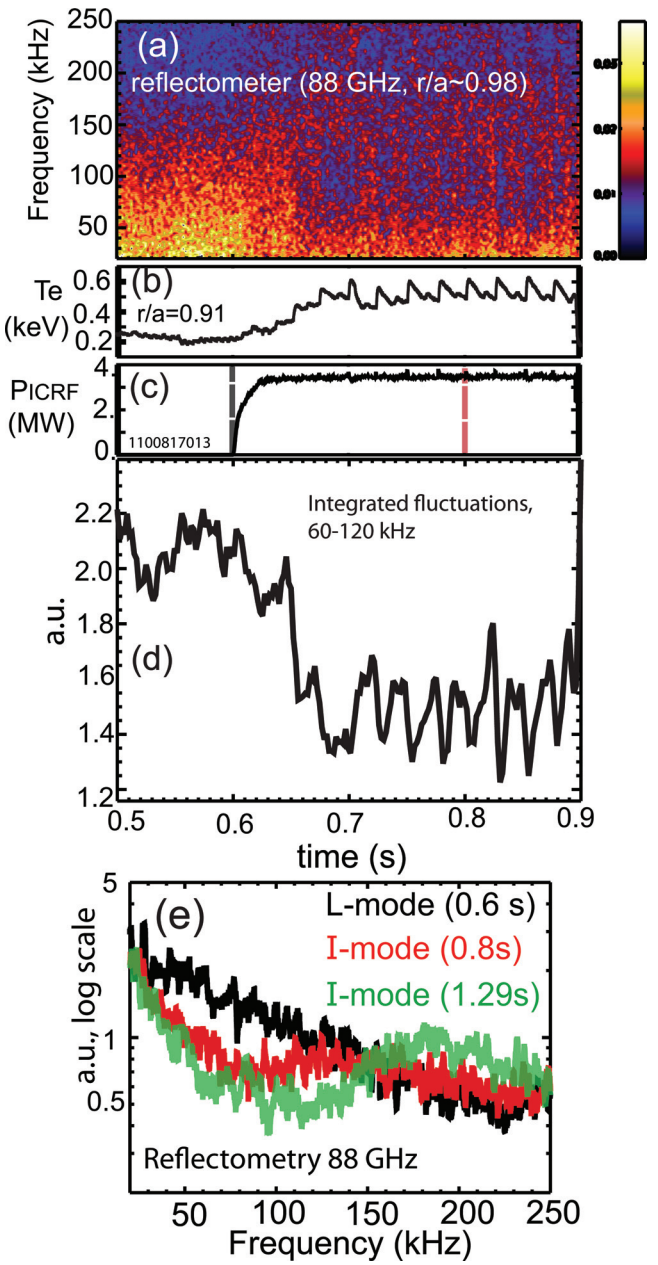

FIG. 6. (Color online) Evolution of fluctuations and edge T_e for a $q_{95} = 3.8$ C-Mod discharge 1100817013 (1.1 MA, 5.6 T, upper single null). (a) Contours of reflectometer fluctuations (88 GHz, $n_c = 9.6 \times 10^{19}$ m^{-3} ($r_c/a \cong 0.98$). (b) T_e at $r/a \cong 0.91$, showing a gradual increase after application of ICRF power (c). (d) Integrated reflectometry fluctuations in the band 60–120 kHz, which are anticorrelated with T_e both during the L–I transition period and at sawtooth heat pulses in the steady I-mode phase. (e) Reflectometry spectra in the L-mode (black) and I-mode phases indicated by bars in (c), and during a later I-mode phase with slightly higher T_e.

B. Edge flows and electric field

Strong shear in edge flows and radial electric field E_r is widely considered to play a key role in the formation of edge particle and energy barriers in the H-mode regime.[23,24] It is thus of interest to compare these quantities in I-mode and H-mode plasmas. Active CXRS data are available on a subset of I-mode discharges, measuring n, T, and velocity profiles of B^{+5} with a diagnostic neutral beam. Initial I-mode investigations focused on discharges with moderate plasma current, 0.8 MA and temperature pedestals (400 eV).[8] Edge ion temperature pedestal profiles were found to be equal to $T_e(r)$, as is typical for most C-Mod plasmas due to the relatively high density and electron–ion coupling. A moderate E_r well of 15 kV/m was observed, with ω_{ExB} intermediate between L- and H-mode regimes. Recent measurements of a higher current I-mode discharge ($I_p = 1.1$ MA, $q_{95} = 3.8$) are shown in Fig. 7. A relatively broad T_i pedestal (width > 1 cm) reaches 500 eV, again equal to $T_e(r)$ (diamonds) within uncertainties. A separate core CXRS diagnostic,[25], not shown, also measures $T_i = T_e$ in the core gradient region into

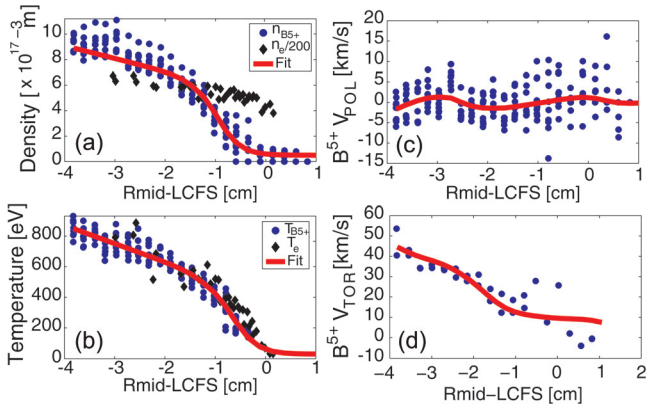

FIG. 7. (Color online) CXRS profiles (circles) for boron + 5, averaged over I-mode phases of the same discharge as in Fig. 6. Note that n_{B+5} (a) does not have the same profile as n_e (black diamonds, scaled by 200 for comparison). Its temperature pedestal (b), however, is the same as T_e measured by edge TS (black diamonds) within respective mapping uncertainties. $V_{\rm pol}$ (c) is flat and near zero, while $V_{\rm tor}$ (d) exhibits co-current rotation of up to 40 km/s.

at least $r/a \sim 0.65$. Toroidal velocity increases from near zero at the separatrix to 45 km/s, in the co-current direction, 4 cm into the confined plasma ($r/a \sim 0.8$), with a profile roughly corresponding to $T_i(r)$. Central toroidal rotation, measured independently from Doppler shifts of core x-ray lines, increases by 70–80 km/s in I-mode, also in the co-current direction. Studies of a large number of I-mode and H-mode discharges have shown that this intrinsic rotation, which can reach 90 km/s, scales with edge ∇T in both regimes.[26] Since I-modes break the usual correlation between T_e, n_e, and p_e gradients, comparisons in this regime have helped to show that there is not a strict correspondence between changes in rotation velocities and edge pressure gradients.

The B^{5+} poloidal rotation velocities are flat across the edge region, and zero within error bars. Comparing contributions to electric field in I-mode to those in a typical EDA H-mode (Fig. 8), the lack of a $V_{\rm pol}$ contribution in the I-mode case [Fig. 8(a)] contrasts with the strong and narrow negative E_r from impurity $V_{pol} \times B_{tor}$ typical of C-Mod H-modes, which has also been measured on some other tokamaks. The net E_r well in I-mode is dominated by the diamagnetic contribution in the impurity force balance, and is 30 kV/m peak-to-peak with a minimum value of –10 kV/m. In contrast, E_r in H-mode [Fig. 8(b)] has a similar diamagnetic contribution but is dominated by the $V_{\rm pol}$ component, giving an E_r well of 65 kV/m peak-to-peak and a lower minimum in the example shown from Ref. 8. EDA H-modes in general tend to have $V_{\rm pol}$ contributions to the E_r well of similar or larger size compared to the diamagnetic contribution.[27]

C. Characteristics of high frequency weakly coherent mode

As evident in Figs. 3, 5, and 6, a key feature of the I-mode regime is the appearance of a high frequency fluctuation peak, at the same time as the decrease in mid-frequency fluctuations and formation of a temperature pedestal. Further details of this "weakly coherent mode" (WCM) are given in Ref. 9. The mode is most clearly and consistently visible on reflectometry, which is sensitive only to density fluctuations. More detailed measurements of the mode location and poloidal wavenumber are obtained from gas puff imaging. As shown in Fig. 9, for an I-mode with $q_{95} = 3.1$ in the unfavorable configuration, the WCM has a typical $k_{\rm pol}$ of $\sim$1–1.5 cm^{-1} and extends over at least 1 cm inside the separatrix, $0.95 < r/a \leq 1$; the inner extent of the diagnostic is limited by the depth of the neutral ionization. Reflectometry confirms the mode is localized to $0.9 < r/a \leq 1$. While these properties are similar to those of the QC mode which causes enhanced particle transport in EDA H-modes,[6] the frequency and thus poloidal phase velocity of the WCM are considerably higher. $V_{\rm pol}$ in the discharge of Fig. 9 is 10.6 ± 1.3 km/s in the electron diamagnetic direction, in the laboratory frame. For the higher q_{95} case shown in Figs. 6–8, $V_{\rm pol}$ of the broader mode is 8.5 ± 3 km/s. Subtracting the weakly positive $V_{E\times B}$ computed from the measured E_r (1.1–2.3 km/s in the region of a maximum WCM amplitude), the velocity in the plasma frame can be estimated as $V_{\rm pol,pl} = 6.8 \pm 3.6$ km/s, still in the electron diamagnetic direction. For comparison, QC modes in EDA typically have $V_{\rm pol}$ 2–4 km/s in the laboratory frame,[22] and given stronger negative E_r will have lower velocity, possibly even in the ion diamagnetic direction, in the plasma frame. Another key distinction between the modes is in their operational space. QC modes and EDA are generally restricted to higher collisionality pedestals, $\nu^*_{\rm ped} > 1$ and obtained most readily at higher q_{95}.[6,28] The WCM, in contrast, is clearest in low q_{95}, high T_e, and low ν^* pedestals; $\nu^*_{\rm ped}$ as low as 0.13 has been achieved to date and there is no sign of a lower limit.[9] Since pedestal temperature and its gradient are highly correlated with I_p in I-modes, it is

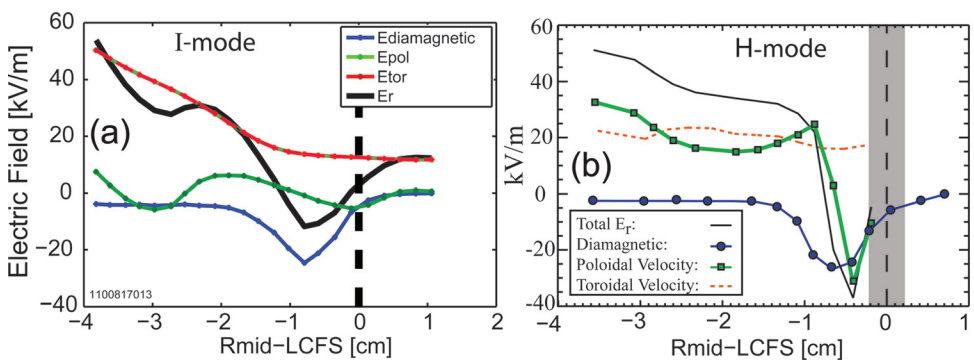

FIG. 8. (Color online) (a) Radial electric field in a 1.1 MA I-mode discharge, derived from the CXRS profiles shown in Fig. 7. The 30 keV/m well in total E_r (black) is dominated by the diamagnetic term (lower curve), with a significant gradient from the $V_{tor} \times B_{pol}$ term (upper curve). (b) For comparison, an E_r profile in a typical EDA H-mode, with $I_p = 800$ kA, which has a stronger contribution from the $V_{pol} \times B_{tor}$ term. Reprinted with permission from McDermott *et al.*, Phys. Plasmas 16, 056103. © 2009, American Institute of Physics.

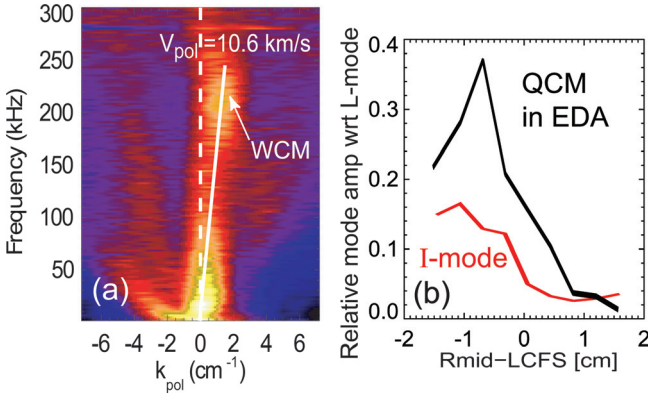

FIG. 9. (Color online) (a) Emission fluctuations measured by gas puff imaging at the horizontal midplane during an I-mode phase of C-Mod discharge 1100204022 (1.3 MA, 5.8 T, upper single null). A weakly coherent mode is visible, centered at about $f = 220$ kHz, $k_{\rm pol} = +1.25$ cm^{-1} (electron diamagnetic direction). (b) Relative amplitude of the WCM (increase over L-Mode turbulence, normalized to average intensity) vs. radius. The radial profile of the quasicoherent mode in an EDA H-mode is shown for comparison (black).

difficult to separate possible dependences of the mode properties. However, as can be seen by comparing Figs. 5 and 6, $\Delta f/f$ is lowest, though still fairly broad, in high current plasmas, e.g., Δf(FWHW) $\cong$ 100 kHz, $\Delta f/f \cong 0.45$, in Fig. 5 at $q_{95} = 3.1$.

In addition to the density fluctuations, a peak at the frequency of the weakly coherent mode is clearly evident on fast magnetic coils, indicating that the responsible turbulence has a significant electromagnetic component. Its measured amplitude is sensitive to the plasma–coil gap, consistent with a short wavelength mode. An estimate of the mode amplitude at the plasma edge, derived from measurements on various magnetic coils for the discharge of Fig. 9 assuming $k_r \sim k_{\rm pol}$, is $3–8 \times 10^{-4}$ T ($\tilde{B}/B_{tot} \sim 0.7–2 \times 10^{-4}$). Typical toroidal mode numbers at this q_{95} (3.1) are $n \cong 20–25$, decreasing to ~ 10 at higher q.

IV. DISCUSSION

I-mode operation clearly demonstrates a regime where energy and particle transport can be separated, that is, where the first can be sharply suppressed while the second remains unchanged. This mode of operation is potentially very attractive for fusion, and may shed light on a number of important issues related to turbulence, transport regulation, and transport bifurcation. A potential picture of thermal transport suppression in the I-mode is emerging. The first step in formation of the barrier is external heating, which increases edge T gradients, both in steady state and more strongly as sawtooth heat pulses propagate to the edge. Edge electric field shear, dominated in both L- and I-modes by the diamagnetic term, increases. This may well be the reason for the observed decrease in mid-frequency turbulence, which has been shown to correlate closely with edge thermal transport, and could enable a further steepening of ∇T. While causality is always difficult to ascertain, the transient reduction in turbulence when edge T rises at each heat pulse in Fig. 6 supports a role of ∇T, or $\nabla p/n_e$, in the suppression. This general picture of a feedback loop leading to transport barrier formation is similar to that proposed for H-modes. However, in this case the changes appear to be rather gradual, with variable time scales for turbulence and transport suppression; intermediate states, difficult to classify as L-mode vs. I-mode, are sometimes observed. This is suggestive of a milder second order transition, with monotonic flux–gradient curves changing in slope, rather than a first order bifurcation (the classic "S-curve") in which transport jumps from one stable state to another.[29] Comparison of CXRS profiles shows that another key difference is that H-modes have a strong $V_{\rm pol}$ shear layer contributing to E_r, whereas E_r in I-modes is dominated by the diamagnetic term. Similar observations of a "two stage H-mode transition" have recently been reported on JT60-U.[30] In the first phase, the T_i and E_r profiles build up gradually, with roughly equal contributions to E_r from diamagnetic and poloidal velocity in the C impurity force balance, and no sharp change in D_α. In the second phase E_r steepens rapidly, dominated by a larger $V_{\rm pol}$ contribution, there is a sharp decrease in D_α, and the change in n_e gradients exceeds that in T_i. It may be that rapid $V_{\rm pol}$ changes are a key part of the usual L–H bifurcation, and that the stronger shear resulting in this case is needed for more complete suppression of turbulence, and of particle transport. However, it should be noted that the velocity profiles of the main ion species will be different from those of the measured impurities.

Key open questions are why the particle transport response to the decrease in mid-frequency turbulence is relatively weak, and why the turbulence at higher frequencies is not suppressed, and often even increases with a well defined peak particularly at low q_{95}. This suggests that energy and particle transport may be dominated by different turbulent modes, k-ranges and/or frequency ranges. The lower E_r shear in I-mode vs. H-mode could then be sufficient to decrease the turbulence responsible for thermal but not particle transport. Another possibility is that changes in phase between n, T, potential ϕ, and B differently affect the energy and particle transport channels.[31] While cross–phase measurements are not currently available, analysis of the response of different diagnostics to the turbulence changes provides some additional information. From the decrease in magnetic fluctuations, the turbulence responsible for thermal transport clearly has an electromagnetic component. Future experiments will aim to assess T_e fluctuations using electron cyclotron emission, which might influence the weaker response on GPI signals, and to compare the changes in density and D_α emission fluctuations in different k ranges.

Other open questions include the physical origin and role of the weakly coherent mode in the I-mode. Given that in some discharges most of the remaining broadband edge turbulence is in this high frequency peak, and that density rises strongly and promptly when this is suppressed at an I–H transition, it seems likely that it plays a role in maintaining or increasing particle transport, and perhaps in avoiding a particle barrier formation. Following this argument, a heavy particle mode has been proposed as a potential instability in this regime.[32] The WCM becomes stronger and more coherent in low q_{95} plasmas with high temperature pedestals; it is not clear which parameter is most important, and further

systematic study is required. It is possible, though by no means demonstrated, that the increased ∇T in I-mode provides a drive for this instability.

Perhaps the most important open issue, with practical implications for potential application to burning plasmas, is in understanding, and ultimately extending and controlling, the conditions in which I-mode, rather than L- or H-mode, can be accessed and robustly sustained. The proximity and overlap between L–I and I–H mode power thresholds implies that I- and H-modes are possible for quite similar global parameters, and that other, probably local, variables play a role. Future research will focus on extending the upper power range for sustaining I-mode without a particle barrier formation. Possible techniques include fueling to higher densities, optimizing shapes to increase the WCM transport, and actively exciting WCM or other edge modes to increase particle transport in the barrier region. Accessing I-mode in a wider range of shapes is also of interest. Experiments on other tokamaks, particularly lower field devices which can more readily assess the pressure limits, will be valuable in extrapolating the conditions and performance of the I-mode regime. While much remains to be learned, the fact that energy and particle transport can vary independently enhances the prospects for their independent control, extremely important for burning plasmas.

V. CONCLUSIONS

The I-mode regime on C-Mod features an edge thermal transport barrier, with T_e and T_i pedestals comparable to those in H-modes, without a strong particle transport barrier. Stationary I-modes have now been obtained with favorable ion $B \times \nabla B$ drift, in specific shapes, at $0.8 \leq I_p \leq 1.0$ MA, $B_T \cong 5.4$ T, as well as with unfavorable drift over a wider range of shape and plasma parameters ($0.7 \leq I_p \leq 1.3$ MA, $3 \leq B_T \leq 6$ T). With favorable drift, power thresholds are close to the standard scaling for L–H transitions, while with unfavorable drift they are ~ 1.5–3 times higher, increasing with I_p. Global energy confinement in both configurations is comparable to that in H-mode ($0.8 < H_{98,y2} < 1.25$), while density profiles and impurity confinement are close to those in L-mode.

Transport analysis of the edge region shows a marked decrease in χ_{eff}, by typically a factor of 3, between L- and I-mode, with a further decrease at the I–H mode transition. The decrease in χ_{eff} correlates well with a decrease in mid-frequency fluctuations on both density and magnetics diagnostics, over a frequency range of ~ 50–150 kHz. Fluctuations at higher frequencies persist and often increase above L-mode levels, with a peak frequency of typically 250 kHz. This weakly coherent mode is strongest and has narrowest width ($\Delta f/f \sim 0.45$) at low q_{95} and high T_{ped}. Impurity CXRS measurements in I-mode reveal an E_r well of typically 30 kV/m peak-to-peak. In contrast to H-mode, there is no V_{pol} component of the B^{+5}, and E_r is dominated by the diamagnetic contribution in the impurity force balance. E_r shear is intermediate between L- and H-mode. Co-current toroidal rotation is observed, scaling with edge ∇T consistent with observations in H-modes.[26] Further research is underway to understand the physics of the edge transport barrier formation, in particular the separation of energy and particle transport. We seek to extend the parameters over which I-mode can be robustly sustained, and to assess the suitability of the regime for burning plasma research, with the ultimate aim of independently controlling the energy and particle confinement.

ACKNOWLEDGMENTS

The authors wish to acknowledge the efforts of the entire Alcator C-Mod team, in particular the ICRF group, in carrying out the experiments reported here. This work was supported by U.S. Department of Energy Contract Nos. DE-FC02-99ER54512 and DE-FG03-96ER54373.

[1]F. Wagner, G. Becker, K. Behringer, D. Campbell, A. Eberhagen, W. Engelhardt, G. Fussmann, O. Gehre, J. Gernhardt, G. V. Gierke, G. Haas, M. Huang, F. Karger, M. Keilhacker, O. Klüber, M. Kornherr, K. Lackner, G. Lisitano, G. G. Lister, H. M. Mayer, D. Meisel, E. R. Müller, H. Murmann, H. Niedermeyer, W. Poschenrieder, H. Rapp, H. Röhr, F. Schneider, G. Siller, E. Speth, A. Stäbler, K. H. Steuer, G. Venus, O. Vollmer, and Z. Yü, Phys. Rev. Lett. **49**, 1408 (1982); F. Wagner, Plasma Phys. Controlled. Fusion **49**, B1 (2007).

[2]E. S. Marmar and Alcator C-Mod Group, Fusion Sci. Technol. **51**(3), 3261 (2007).

[3]M. Shimada, D. J. Campbell, V. Mukhavatov, M. Fujiwara, N. Kirneva, K. Lackner, M. Nagami, V. D. Pustovitov, N. Uckan, J. Wesley, and ITPA Topical Group Chairs, Nucl. Fusion **47**, S1 (2007).

[4]H. Zohm, Plasma Phys. Controlled Fusion **38**(2), 105 (1996).

[5]A. Loarte, B. Lipschultz, A. S. Kukushkin, G. F. Matthews, P. C. Stangeby, N. Asakura, G. F. Counsell, G. Federici, A. Kallenbach, K. Krieger, A. Mahdavi, V. Philipps, D. Reiter, J. Roth, J. Strachan, D. Whyte, R. Doerner, T. Eich, W. Fundamenski, A. Herrmann, M. Fenstermacher, P. Ghendrih, M. Groth, A. Kirschner, S. Konoshima, B. LaBombard, P. Lang, A. W. Leonard, P. Monier-Garbet, R. Neu, H. Pacher, B. Pegourie, R. A. Pitts, S. Takamura, J. Terry, E. Tsitrone and the ITPA Scrape-off Layer and Divertor Physics Topical Group, Nucl. Fusion **47**, S203 (2007); A. Loarte, D. J. Campbell, Y. Gribov, R. A. Pitts, N. Klimov, V. Podkovyrov, A. Zhitlukhin, I. Landman, S. Pestchanyi, B. Bazylev, J. Linke, T. Loewenhoff, G. Pintsuk, O. Schmitz, Y. Liang, T. E. Evans, M. Schaffer, M. E. Fenstermacher, M. Becoulet, G. Huysmans, E. Nardon, L. Baylor, J. Canik, R. Maingi, J. W. Ahn, B. Riccardi, G. Saibene, R. Sartori, M. Cavinato, T. Eich, M. Jakubowski, P. T. Lang, H. Thomsen, W. Suttrop, E. De la Luna, H. Wilson, and A. Kirk, Fusion Energy Conference 2010, Seoul, Korea, Paper ITR/1–4,

[6]M. Greenwald, R. Boivin, P. Bonoli, R. Budny, C. Fiore, J. Goetz, R. Granetz, A. Hubbard, I. Hutchinson, J. Irby, B. LaBombard, Y. Lin, B. Lipschultz, E. Marmar, A. Mazurenko, D. Mossessian, T. Sunn Pedersen, C. S. Pitcher, M. Porkolab, J. Rice, W. Rowan, J. Snipes, G. Schilling, Y. Takase, J. Terry, S. Wolfe, J. Weaver, B. Welch, and S. Wukitch, Phys. Plasmas **6**(5), 1943 (1999).

[7]K. H. Burrell, M. E. Austin, D. P. Brennan, J. C. DeBoo, E. J. Doyle, P. Gohil, C. M. Greenfield, R. J. Groebner, L. L. Lao, T. C. Luce, M. A. Makowski, G. R. McKee, R. A. Moyer, T. H. Osborne, M. Porkolab, T. L. Rhodes, J. C. Rost, M. J. Schaffer, B. W. Stallard, E. J. Strait, M. R. Wade, G. Wang, J. G. Watkins, W. P. West and L. Zeng, Plasma Phys. Controlled Fusion **44**, A253 (2002).

[8]R. McDermott, B. Lipschultz, J. W. Hughes, P. J. Catto, A. E. Hubbard, I. H. Hutchinson, R. S. Granetz, M. Greenwald, B. LaBombard, K. Marr, M. L. Reinke, J. E. Rice, D. Whyte, and Alcator C-Mod Team, Phys. Plasmas **16**, 056103 (2009).

[9]D. G. Whyte, A. E. Hubbard, J. W. Hughes, B. Lipschultz, J. E. Rice, E. S. Marmar, M. Greenwald, I. Cziegler, A. Dominguez, T. Golfinopoulos, N. Howard, L. Lin, R. M. McDermott, M. Porkolab, M. L. Reinke, J. Terry, N. Tsujii, S. Wolfe, S. Wukitch, Y. Lin, and the Alcator C-Mod Team, Nucl. Fusion **50**, 105005 (2010).

[10]M. Greenwald, R. L. Boivin, F. Bombarda, P. T. Bonoli, C. L. Fiore, D. Garnier, J. A. Goetz, S. N. Golovato, M. A. Graf, R. S. Granetz, S. Horne, A. Hubbard, I. H. Hutchinson, J. H. Irby, B. LaBombard, B. Lipschultz, E. S. Marmar, M. J. May, G. M. McCracken, P. O'Shea, J. E. Rice, J.

Schachter, J. A. Snipes, P. C. Stek, Y. Takase, J. L. Terry, Y. Wang, R. Watterson, B. Welch, S. M. Wolfe, Nucl. Fusion **37**(6), 793 (1997).
[11]F. Ryter, W. Suttrop, B. Brusehaber, M. Kaufmann, V. Mertens, H. Murmann, A. G. Peeters, J. Stober, J. Schweinzer,H. Zohm, and ASDEX Upgrade Team, Plasma Phys. Controlled Fusion **40**, 725 (1998).
[12]R. J. Groebner and T. N. Carlstrom, Plasma Phys. Controlled Fusion **40**, 673 (1998); T. N. Carlstrom, K. H. Burrell, and R. J. Groebner, Plasma Phys. Controlled Fusion **40**, 669 (1998).
[13]A. Hermann and O. Grüber, Fusion Sci. Technol. **44**, 569 (2003).
[14]A. E. Hubbard. J. W. Hughes, I. O. Bespamyatnov, T. Biewer, I. Cziegler, B. LaBombard, Y. Lin, R. McDermott, J. E. Rice, W. L. Rowan, J. A. Snipes, J. L. Terry, S. M. Wolfe, S. Wukitch, and Alcator C-Mod Group, Phys. Plasmas **14**(5), 056109 (2007).
[15]A. E. Hubbard, B. A. Carreras, R. L. Boivin, J. W. Hughes, E. S. Marmar, D. Mossessian, and S. J. Wukitch, Plasma Phys. Controlled Fusion **44**, A359 (2002).
[16]A. E. Hubbard, B. A. Carreras, N. P. Basse, D. del-Castillo-Negrete, J. W. Hughes, A. Lynn, E. S. Marmar, D. Mossessian, P. Phillips, and S. Wukitch, Plasma Phys. Controlled Fusion **466**(5), A95 (2004).
[17]Y. Martin, T. Takizuka, and ITPA CDBM H-mode Threshold Database Working Group, J. Phys. Conf. Ser. **123**, 012033 (2008).
[18]ITER Physics Expert Groups on Confinement and Transport and Confinement Modelling and Database, ITER Physics Basis Editors, and ITER EDA, Nucl. Fusion **39**, 2175 (1999).
[19]J. W. Hughes, A. Loarte, M. L. Reinke, J. L. Terry, D. Brunner, A. E. Hubbard, B. LaBombard, B. Lipschultz, J. Payne, S. Wolfe, S. J. Wukitch, Fusion Energy Conference 2010, Seoul, Korea, paper EXC/P3-06TR/1—4 Nucl. Fusion (submitted).
[20]J. W. Hughes, D. A. Mossessian, A. E. Hubbard, E. S. Marmar, D. Johnson, and D. Simon, Rev. Sci. Instrum. **72**, 1107 (2001).
[21]Y. Lin, R. Nazikian, J. H. Irby, and E. S. Marmar, Plasma Phys. Controlled Fusion **43**, L1 (2001).
[22]I. Cziegler, J. L. Terry, J. W. Hughes, and B. LaBombard, Phys. Plasmas **17**, 056120 (2010).
[23]K. H. Burrell, Phys. Plasmas **4**(5), 1499 (1997).
[24]H. Biglari, P. H. Diamond, and P. W. Terry, Phys. Fluids B **2**(1), 1 (1990).
[25]W. L. Rowan, I. O. Bespamyatnov, and R. S. Granetz, Rev. Sci. Instrum. **79**, 10F529 (2008).
[26]J. E. Rice, J. W. Hughes, P. H. Diamond, Y. Kosuga, Y. A. Podpaly, M. L. Reinke, M. J. Greenwald, O. D. Gurcan, T. S. Hahm, A. E. Hubbard, E. S. Marmar, C. J. McDevitt, and D. G. Whyte, The edge temperature gradient as intrinsic rotation drive in Alcator C-Mod tokamak plasmas, Phys. Rev. Lett. (to be published).
[27]R. McDermott "Edge radial electric field studies via charge-exchange recombination spectroscopy on the Alcator C-Mod tokamak," Ph.D. thesis (Massachusetts Institute of Technology, Cambridge, MA, 2009).
[28]J. W. Hughes, A. E. Hubbard, D. A. Mossessian, B. LaBombard, T. M. Biewer, R. S. Granetz, M. Greenwald, I. H. Hutchinson, J. H. Irby, Y. Lin, E. S. Marmar, M. Porkolab, J. E. Rice, J. A. Snipes, J. L. Terry, S. Wolfe, and K. Zhurovich, Fusion Sci. Technol. **51**(3), 317 (2007).
[29]J. W. Connor and H. R. Wilson, Plasma Phys. Controlled Fusion **42**, R1 (2000). See also references therein.
[30]K. Kamiya, K. Ida, Y. Sakamoto, G. Matsunaga, A. Kojima, H. Urano, N. Oyama, Y. Koide, Y. Kamada, and JT-60 Team, Phys. Rev. Lett. **105**, 045004 (2010).
[31]A. S. Ware, P. W. Terry, B. A. Carreras, and P. H. Diamond, Phys. Plasmas **5**(1), 173 (1998).
[32]B. Coppi and T. Zhou, "Heavy particle modes and signature of the I-regime," MIT (LNS) Report HEP-09/04 (Cambridge, November 2009); (submitted to Physics Letters A, 2011)